

## Structure and motion of inter-ELM filaments in MAST

N. Ben Ayed<sup>1,2</sup>, B. Dudson<sup>1,2</sup>, A. Kirk<sup>2</sup>, R. G. L. Vann<sup>1</sup>, H. R. Wilson<sup>1</sup>, S. Tallents<sup>2</sup>  
and the MAST team<sup>2</sup>.

<sup>1</sup>*Department of Physics, University of York, Heslington, York, YO10 5DD, U.K.*

<sup>2</sup>*UKAEA Fusion Association, Culham Science Centre, Abingdon, Oxfordshire, U.K.*

In recent years, edge filamentary structures across a wide range of magnetically confined plasmas have received much attention<sup>1-4</sup>, since it is believed that the dynamics of these field-aligned entities dominate the radial transport and flow in the scrape-off layer (SOL). In the case of the Mega Ampère Spherical Tokamak, this characteristic filamentary nature is best displayed with a midplane-mounted, fast-framing visible camera: the Photron Ultima APX-RS camera is used to continuously capture a set of images at varying frequencies and exposure times. In the low confinement mode (L-mode) on MAST, these turbulence-driven structures are significantly more dense than the background plasma (See Fig. 1(a)) and project a large distance from the last closed flux surface<sup>5</sup> (LCFS). Furthermore, during high confinement modes (H-mode), the edge transport barrier is quasi-periodically destroyed by edge localised modes (ELMs). These relaxations of the edge plasma density and temperature profiles involve the formation of localised filaments (see Fig. 1(b)) with particle densities and temperatures characteristic of the plasma pedestal<sup>5,6</sup>. Whilst previous efforts have been dedicated to the study of L-mode and ELM filaments<sup>5</sup>, few efforts have concentrated on the period between ELMs<sup>7</sup>; namely, the inter-ELM phase. As is shown by the single frame in Fig. 1(c), this period may seem to be filament-free; however, background subtraction reveals a remarkable filamentary nature similar to both L-mode and ELM phases. In this paper, the physical properties of inter-ELM filaments are presented.

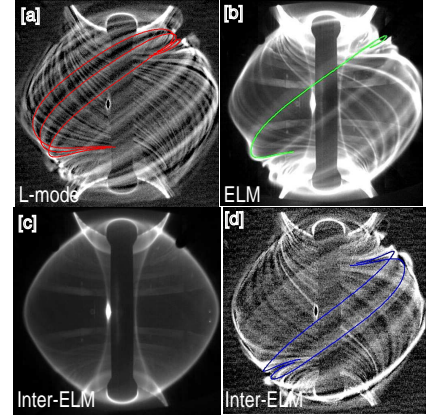


Figure 1: Sequence of visible images during [a]: L-mode, [b]: ELM, [c]: inter-ELM and [d]: inter-ELM with background subtraction.

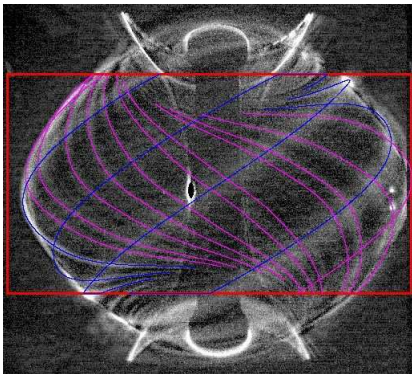


Figure 2: Full view of inter-ELM plasma showing all filaments effectively localised.

of this technique applied to an inter-ELM frame where foreground and background filaments, marked by the red and blue lines respectively, are localised. It is immediately

Filaments are localised by projecting 3D field lines, generated from the magnetic equilibrium in 1cm steps outside the LCFS, onto the 2D images. Radial positions are determined by choosing the best fit between the mapped field line and the observed filament. In the case of inter-ELM filaments, this is assumed to be at the LCFS. In order to localise all the filaments that span a toroidal angle  $\Delta\phi$ , this procedure is repeated in  $0.5^\circ$  steps whilst measuring the average intensity,  $\bar{I}$ , along each mapped field line. The toroidal locations of the filaments are subsequently given by unfolding the total intensities,  $I_{tot} = \sum_{i=0}^{i=\Delta\phi} \bar{I}(\Delta R_{LCFS}, i)$ , corresponding to all mapped field lines and applying suitable peak detection algorithms. Fig. [2] shows an example

obvious that, in common with L-mode and ELM phases, filaments during inter-ELM periods are also aligned with the local field lines.

The technique described above is used to derive a quantitative description of the temporal evolution of filaments during a typical inter-ELM period, shown in Fig. 3[a]. This is best achieved using narrow views of the midplane with a spatial resolution of  $128 \times 48$  pixels (shown in Fig. 3) at a framing rate of 100kHz with an integration time of  $10\mu\text{s}$ . Fig. 3[a] shows the spatial evolution of detected filaments which span the range of  $160\text{--}270^\circ$  in toroidal angle. The trajectories of individual filaments are tracked by joining intensity-correlated peaks and are marked by continuous lines. They are found to remain in the immediate vicinity of the LCFS, i.e.  $\Delta R_{LCFS} \leq 2\text{cm}$ , whilst continuously rotating toroidally in the co-current direction. Moreover, the filaments rotate by a constant  $3 - 5^\circ$  every  $10\mu\text{s}$  which corresponds to a toroidal velocity in the range between  $7.5\text{--}12.5\text{ km/s}$ . The inter-ELM filaments are typically observed to be long-lived phenomena with lifetimes,  $\tau$ , in the range  $50 \sim 120\mu\text{s}$ . This is considerably longer than the electrostatic turbulence-driven L-mode filaments ( $\tau \leq 50\mu\text{s}$ ).

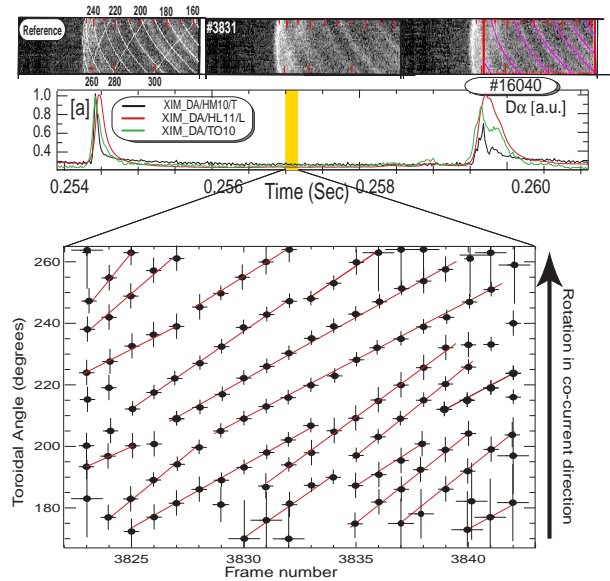


Figure 3: Temporal evolution of detected filaments in the toroidal range  $160\text{--}270^\circ$ . Trajectories of individual filaments are marked by continuous lines.

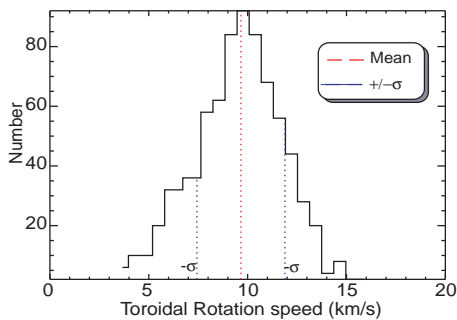


Figure 4: Histogram of the number of filaments as a function of toroidal velocity.

In an attempt to establish a dependence of filament motion on various plasma parameters, the toroidal rotation has been tracked in plasmas with a wide variety of parameters involving the toroidal field  $B_T = 0.45 - 0.6T$ , plasma current  $I_p = 600 - 1100\text{ kA}$  and neutral beam heating power  $P_{NBI} = 1 - 3.2\text{ MW}$ . The histogram presented in Fig. 4 shows no significant changes in the toroidal rotation despite the large range of plasma parameters covered. It is interesting to note that though the filaments in L-mode, ELM and inter-ELM periods are characterised by distinct propagation speeds, the lack of parameter dependence within each class of filament is a common feature.

An estimate of the filament widths,  $L_\perp$ , may be obtained from the width of the peak in  $D_\alpha$  emission normal to the mapped field. An examination of 2000 filaments yields a range of perpendicular widths (FWFM) between 15 and 45 cm with a mean width,  $\bar{L}_\perp \sim 30\text{ cm}$ . A similar analysis for L-mode filaments yields a range between 5 and 20 cm. In addition, a survey of the average spacing of the filaments leads to quasi toroidal mode numbers,  $n_{ielm}$ , in the range between 10-40 with a mean,  $\bar{n}_{ielm} \sim 25$  for inter-ELM filaments, and a range of 30-50 with  $\bar{n}_{lmode} \sim 45$  for L-mode filaments.

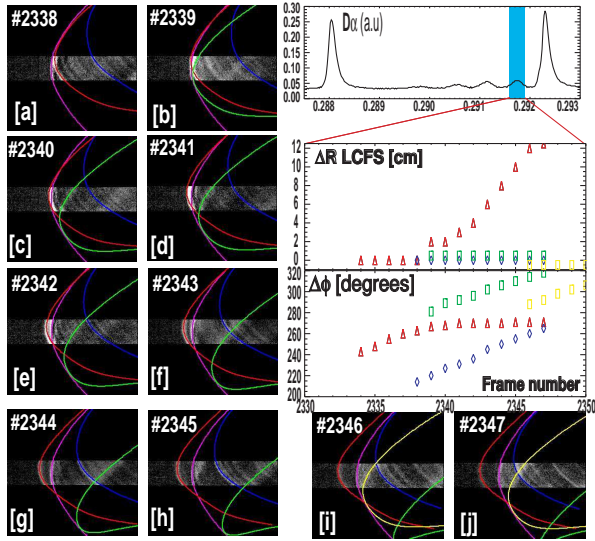


Figure 5: *Radial expulsion of an inter-ELM filament.*

that it is no longer attached to the plasma at the midplane. During this process, neighbouring filaments are largely unaffected and continue to rotate for at least the duration of the radial expansion. The two-fold nature of the motion bears a strong similarity with ELM behaviour<sup>8</sup>; however, this similarity is weakened by the non-global nature of this phenomenon since radial expansions seldom involve more than a few filaments.

The outboard midplane reciprocating probe (RP) system is equipped with a circular array of 8 equally spaced, flush mounted Langmuir probes arranged in diametrically opposite pairs, as shown in Fig. 6. These probes are operated in the ion saturation regime, and measure the ion saturation current,  $I_{sat}$ . A sample of the time series in an inter-ELM period, illustrated in Fig. (6) [c-d] reveals the existence of a number of intermittent peaks against a high frequency background. As shown in Fig. (6)[e], each peak is correlated with a filament crossing the probe. It is found that the burst of  $I_{sat}$  during these periods varies with the distance of the probe from the plasma edge: the highest  $I_{sat}$  frequency and amplitudes are recorded at the LCFS,  $\Delta R_{LCFS} \leq 2\text{cm}$ , and nearly vanish when beyond  $\Delta R_{LCFS} \geq 3\text{cm}$ . This is in agreement with the observation made earlier by fast imaging that most inter-ELM filaments remain very close to the separatrix.

A comparison of L-mode, ELM and inter-ELM  $I_{sat}$  values taken at the LCFS is shown in Fig. 7. The highest values of  $I_{sat}$  correspond to the ELM transients whereas the lowest values are associated with inter-ELM filaments which are consistently below the L-mode

Whilst filaments during inter-ELM periods remain on the whole close to the LCFS  $\Delta R_{LCFS} \leq 2\text{cm}$ , with a dominantly toroidal motion; it is found that they do sporadically propagate radially outwards; i.e.  $\Delta R_{LCFS} \geq 2\text{cm}$ . The motion of such filaments is markedly different from the previous description, and is exemplified in Fig. 5 [a-j] where we reconstruct radial  $\Delta r$ , and toroidal steps,  $\Delta\phi$ , of one such filament and immediate neighbours. The filament, marked by the red field line, initially rotates near the LCFS for the first 50  $\mu\text{s}$ ; soon after this, the toroidal rotation slows and as it does so it accelerates radially outwards traversing the LCFS (marked by the magenta line) such

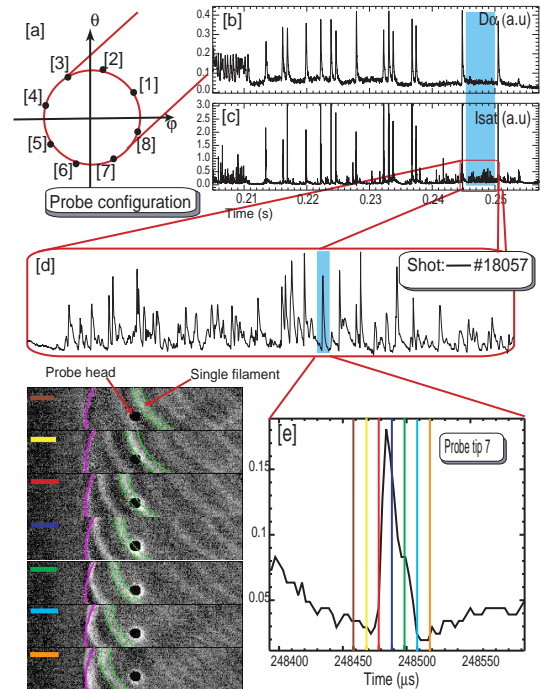


Figure 6: *Sample time series of  $I_{sat}$ . Peaks are confirmed by fast imaging to be filaments.*

values. Quantitatively,  $\langle I_{sat} \rangle_{ielm} \sim 0.15A \leq \langle I_{sat} \rangle_{lmode} \sim 0.45A \leq \langle I_{sat} \rangle_{elm} \sim 1.45A$ . A density for the inter-ELM filament may be given. Assuming equal ion and electron temperatures,  $T_i = T_e$  for the probe collecting area, and that  $T_e$  is in the range  $10 - 25eV$ , based on 160 inter-ELM profiles obtained from the edge Thomson Scattering system<sup>5</sup>, a density is found to be in the range between  $5 \times 10^{17} \rightarrow 2 \times 10^{18} m^{-3}$ .

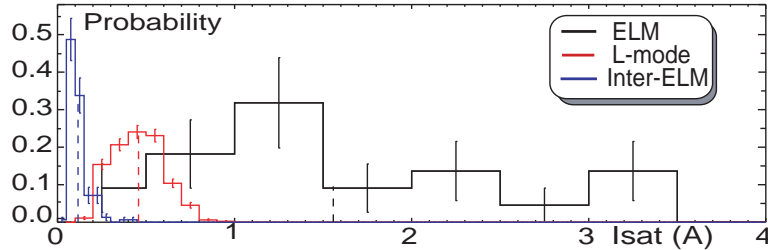
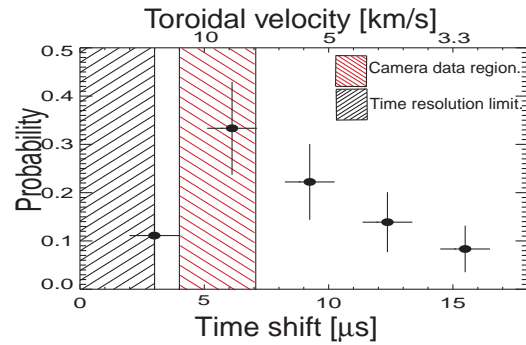


Figure 7: Comparison of L-mode, ELM and Inter-ELM  $I_{sat}$  values at the LCFS.

Finally, from the time shift of signals at neighbouring probe tips,  $\Delta\tau$ , and the separation of the tips,  $\Delta r$ , toroidal velocities of fluctuations  $v_{tor} = \Delta r / \Delta\tau$  can be deduced. In Fig 8. the time shifts measured for two diametrically opposing tips (1 & 5) are shown. The calculated toroidal velocities are compatible with the estimates from the fast camera (marked by the red cross-hatched region).



In summary, analysis of fast camera images reveals the existence of extended filamentary structures during inter-ELM periods in MAST

plasmas. These filaments are observed to be field-aligned quantities, with typical mode numbers of 20-30, lasting for  $\sim 50-120 \mu s$ . The significant reduction in edge turbulence is portrayed through the lack of observed radial transport during these periods since filaments are found to rotate in the co-current direction, with speeds in the range between 7-12km/s. A comparison of ion saturation currents from reciprocating Langmuir probe signals taken at the LCFS show that filaments in inter-ELM periods have a density in the range between  $5 \times 10^{17} \rightarrow 2 \times 10^{18} m^{-3}$  which is lower than L-mode and ELM filaments. Radially propagating filaments during inter-ELM periods are sporadically observed. The two-fold nature of the motion of these filaments is markedly different from the conventional scenario of continuous rotation, and bears the features of ELM propagation<sup>8</sup>.

Figure 8: Time shifts of  $I_{sat}$  peaks in tips 1 & 5.

[1] Kirk A et al., *Plasma Phys. Control. Fusion* **47** 315-333 (2005).

[2] Grulke O et al., *Phys. Plasmas* **13** 012306-1 (2005).

[3] Rudakov D L et al., *Nucl. Fusion* **45** 1589 (2005).

[4] Zweben S J et al., *Phys. Plasmas* **13** 056114 (2005).

[5] Scannell R et al., *Plasma Phys. Control. Fusion* To be published. **12** 062309 (2005).

[6] Kirk A et al., *Plasma Phys. Control. Fusion* **48** B433-B441 (2006)

[7] Alonso J A et al., *Plasma Phys. Control. Fusion* **48** B465-B473 (2006).

[8] Kirk A et al., *Plasma Phys. Control. Fusion* To be published.

*This work was funded in part by the United Kingdom Engineering and Physical Sciences Research Council and by EURATOM. The views and opinions expressed here-in do not necessarily reflect those of the European Commission.*